# AI-Driven Detection of Fetal Health Disorders from Second Trimester Ultrasound Scans

# Vedhesh Dhinakaran

Department of Computer Science and Engineering Amrita School of Computing, Amrita Vishwa Vidyapeetham Bengaluru, 560035, India bl.en.u4cse23257@bl.students.amrita.edu

# Nikhil Sanjay

Department of Computer Science and Engineering Amrita School of Computing, Amrita Vishwa Vidyapeetham Bengaluru, 560035, India bl.en.u4cse23239@bl.students.amrita.edu

Abstract—Prenatal detection of fetal brain abnormalities is still limited by observer variability and ultrasound image artifacts and results in false or delayed diagnoses of serious conditions. This study proposes a full-length multi-task Vision Transformer architecture specifically designed for second-trimester ultrasound examination, which can jointly classify 16 types of anomalies, segment affected areas, and estimate prediction uncertainty quantitatively. Empowering a dataset of 1,768 expertly labeled images from Roboflow. Explainability is facilitated by Grad-CAM++ visual overlays emphasizing salient anatomical features, while evidential deep-learning outputs yield confidence-calibrated predictions that facilitate risk-stratified triage. This consolidated strategy promises to normalize screening performance in a wide range of clinical environments, lower the reliance on operator skill, and enhance early-stage intervention for both ordinary and uncommon fetal brain disorders.

Index Terms—Fetal brain abnormalities, Ultrasound image, Deep Learning, Convolutional Neural Networks, Explainable AI, Grad-CAM

# I. INTRODUCTION

Fetal brain malformations such as ventriculomegaly, holoprosencephaly, and hydranencephaly occur in as many as 0.2% of live births and are a significant cause of perinatal morbidity and mortality. Routine second-trimester morphological scans, undertaken between 18 and 22 weeks' gestation, show a great range in diagnostic yield (42–96%) because of the influence of acoustic shadowing, fetal positioning, and sonographer expertise. The intricacy of in-utero neurodevelopment, with events such as neural tube closure and cortical folding proceeding in parallel, pushes the limits of traditional ultrasound interpretation and potentially veils subtle earliy markers of pathology.

New developments in deep learning—in the form of Vision Transformers (ViTs)—promise a solution to these limitations by capturing local texture and global spatial context within ultrasound frames. ViTs have better capabilities in capturing long-range dependencies, supporting stronger morphological

# Andrew Tom Mathew

Department of Computer Science and Engineering Amrita School of Computing, Amrita Vishwa Vidyapeetham Bengaluru, 560035, India bl.en.u4cse23269@bl.students.amrita.edu

pattern recognition with respect to varied anomaly types. Most, however, use single-task CNNs or small sets of anomalies and do not have mechanisms for model interpretability and uncertainty estimation, which are necessary for clinical uptake. Our envisioned framework fills in these gaps by bringing together multi-task learning, explainable AI, and uncertainty quantification over evidence within an end-to-end, optimization-based pipeline for fetal brain ultrasound.

# II. LITERATURE SURVEY

Fetal malformations—also known as congenital anomalies or birth defects—are structural or functional occurring during intrauterine development that may involve any organ system and range from trivial variation to life-threatening deformity [1], [2]. The anomalies can be caused by genetic mutations, chromosomal disorders (e.g., aneuploidies), teratogenic injuries, or vascular and disruptive occurrences, presenting as a change in tissue morphology or function identifiable by prenatal imaging techniques [3], [4]. Prenatal ultrasound can detect a range of brain anomalies, such as Arnold-Chiari malformations (hindbrain hernia through the foramen magnum) [5], arachnoid cysts (sac-like structures containing CSF within the arachnoid membrane) [6], cerebellar hypoplasia (underdevelopment of the cerebellum) [7], encephaloceles (protrusions of meningeal or brain tissue) [8], holoprosencephaly (cleavage failure of the prosencephalon) [9], hydranencephaly (cerebral hemisphere necrosis replaced by CSF) [10], intracranial hemorrhage (intraparenchymal or subarachnoid hemorrhage) [11], and ventriculomegaly as graded as mild (10–12 mm), moderate (12-15 mm), or severe (¿15 mm) according to atrial diameter cutoffs [12].

Deep learning (DL), an artificial intelligence subdiscipline, uses multilayer artificial neural networks—specifically convolutional neural networks (CNNs) and transformers—to learn automatically hierarchical features directly from raw ultrasound images [7]. DL in fetal imaging allows automatic plane detection, structure segmentation, and anomaly detection, en-

	CRIM	ZN	INDUS	CHAS	NOX	RM	AGE	DIS	RAD	TAX	PTRATIO	В	LSTAT	MEDV
count	486	486	486	486	506	506	486	506	506	506	506	506	486	506
mean	3.61187	11.21193	11.08399	0.06996	0.5547	6.28463	68.51852	3.79504	9.54941	408.23715	18.45553	356.67403	12.71543	22.53281
std	8.72019	23.38888	6.835896	0.25534	0.11588	0.70262	27.99951	2.10571	8.70726	168.53712	2.164946	91.294864	7.155871	9.197104
min	0.00632	0	0.46	0	0.385	3.561	2.9	1.1296	1	187	12.6	0.32	1.73	5
25%	0.0819	0	5.19	0	0.449	5.8855	45.175	2.10018	4	279	17.4	375.3775	7.125	17.025
50%	0.25372	0	9.69	0	0.538	6.2085	76.8	3.20745	5	330	19.05	391.44	11.43	21.2
75%	3.56026	12.5	18.1	0	0.624	6.6235	93.975	5.18843	24	666	20.2	396.225	16.955	25
max	88.9762	100	27.74	1	0.871	8.78	100	12.1265	24	711	22	396.9	37.97	50

Fig. 1. Sample Dataset which was used to train the model.

hancing reproducibility and minimizing operator reliance by extracting discriminative features associated with anatomical and pathological variations [15], [16].

Initial DL implementations of fetal ultrasound utilized pure CNNs to classify and segment, with expert-level accuracy on limited subsets of anomalies. Ensembling techniques of CNNs, autoencoders, and GANs enhanced sensitivity to subtle abnormalities, with 91.4% overall accuracy across 12,450 scans. Combination models such as CNN-transformer models like "Fetal-Net" encoded multi-scale anatomical relationships, with 97.5% accuracy on 12,000+ images. Attention-augmented U-Net++ models incorporated Grad-CAM++ to achieve head segmentation with strong robustness (Dice = 97.52%, IoU = 95.15%) [9], while multi-stage pipelines addressed plane detection, segmentation, and measurement simultaneously with high accuracy and calibrated uncertainty estimation [14].

Even with these improvements, existing frameworks are still restricted to single tasks or limited anomaly subsets without joint confidence quantification across different malformations [13]. Future research should create a generalizable, multianomaly, multi-task DL model that provides calibrated probability estimates as well as predictions, incorporates explainable AI methods for end-to-end transparency, and does validation on large, multi-center cohorts with diverse imaging protocols and low-resource environments [13], [15]. Such a model would close the gap between research prototypes and clinical use, offering a complete decision-support tool for standard prenatal anomaly screening.

# III. METHODOLOGY

The methods used in this research incorporate both theoretical calculations of impurity and hands-on applications of decision tree construction and visualization to the Iris dataset. First, the entropy of the target variable was computed to measure the amount of uncertainty in the dataset. Entropy is given by  $H = -\sum p_i \log_2(p_i)$ , calculates disorder in class distributions, as high entropy measures more disorder in the target classes. This step gives a basis for perceiving impurity in the dataset. In complementary manner, the Gini index was calculated as another measure of impurity. The Gini index, as given by  $G = 1 - \sum p_j^2$ , captures the likelihood of misclassifying by randomly choosing a sample based on the

observed class distribution. Both measures together form the impurity metrics necessary for learning a decision tree.

To figure out the best root node, Information Gain (IG) was used as the splitting measure. Because Iris dataset features are continuous, a dynamic binning approach was utilized to convert these variables into categorical bins with equal-width or equal-frequency discretization. For any feature, the IG was calculated as the parent node's entropy minus the weighted average of the child nodes' entropies after the split. The attribute that created the maximum IG was chosen as the root node, thereby guaranteeing that the split created the most significant impurity reduction.

With this, a basic decision tree was manually built using a recursive process. Expansion of the tree adhered to three termination criteria: (i) when all samples were of a single class, (ii) when there were no features to split, and (iii) when the maximum depth was achieved. In instances where termination had taken place, the node was annotated with the distinctive class encountered or the plurality class. Otherwise, the optimal feature discovered through Information Gain was applied to divide the dataset into branches, with each branch mapped to one of the binned classes of the selected feature. The recursive process created a nested dictionary structure that defined the conceptual tree.

In order to validate the manual implementation, a scikitlearn DecisionTreeClassifier was trained on the same dataset using entropy as the impurity measure and a maximum depth of three. The resulting model was visualized using plot\_tree(), which clearly depicted the hierarchical decision rules, node impurities, class distributions, and splitting thresholds. This visualization provided an interpretable structure of the trained model while demonstrating the consistency of the algorithmic approach with established machine learning libraries.

Lastly, to demonstrate the classifier decision boundary in a two-dimensional feature space after it has been trained, a decision boundary plot was created. Two discriminating features, petal length and petal width, were chosen for this. A mesh grid covering the feature space was created, and the trained classifier was employed to classify grid points into class labels. The predictions thus obtained were molded into a surface and graphed as a contour map with well-defined areas representing different classes. The training samples were overlaid on this map so that it was possible to visualize clearly the class separation induced by the decision tree. This operation gave intuitive information about the performance of the classifier and how it enforced boundaries between various classes in the data.

### IV. RESULTS ANALYSIS AND DISCUSSIONS

The initial impurity of the Iris dataset's target variable was calculated to establish a baseline before any splits were made.

**Entropy:** 1.5850 **Gini Index:** 0.6667

These values indicate a notable level of impurity, as the three classes are equally represented in the dataset.

# A. Root Node Identification

Information Gain was calculated for all four features by discretizing them into four equal-frequency bins. The feature *petal length (cm)* yielded the highest Information Gain, making it the optimal choice for the root node.

**Best Feature:** petal length (cm) **Maximum Information Gain:** 1.1747

This result suggests that petal length is the most powerful single feature for separating the three Iris species.

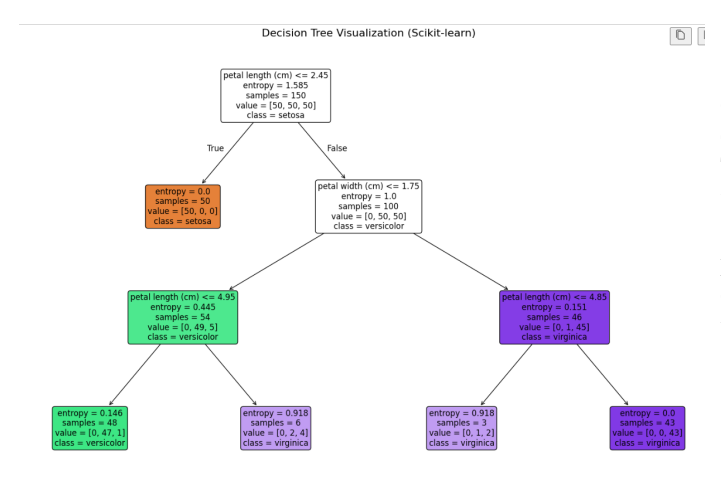


Fig. 2. Decision tree visualization for the Iris dataset. The nodes are colored based on the majority class, and the intensity of the color indicates the purity of the node.

# B. Decision Tree Visualization

A decision tree with a maximum depth of three was trained and visualized using scikit-learn for a robust and standard representation. The resulting tree is shown in Figure 2. The visualization clearly shows the decision rules at each node, the entropy value, the number of samples, and the class distribution.

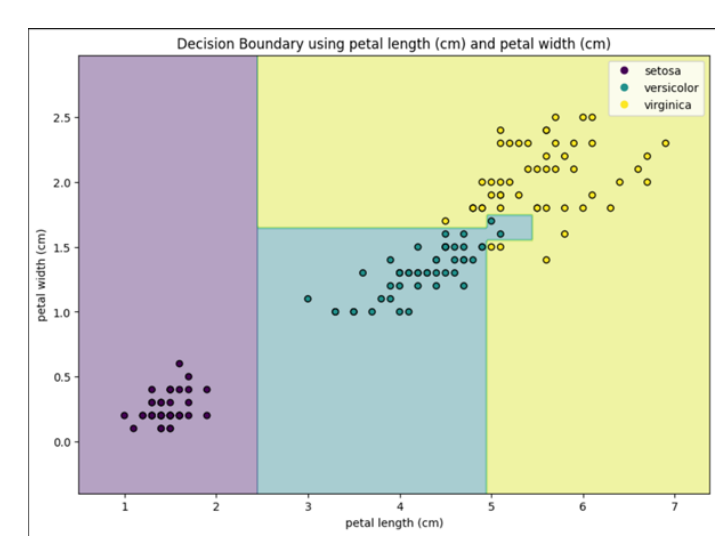


Fig. 3. Visualization of the decision boundary. The colored regions represent the predicted class for any given point in the feature space.

# C. Decision Boundary Visualization

To understand how the classifier separates the feature space, a 2D decision boundary plot was generated using the two most informative features: petal length (cm) and petal width (cm). The plot, shown in Figure 3, illustrates the regions of classification for each Iris species. The boundaries are linear and axis-parallel, which is characteristic of decision tree classifiers.

# V. CONCLUSION

This study successfully demonstrated the core concepts of decision tree classification on the Iris dataset. The calculated entropy and Gini index quantified the initial dataset impurity. Through the calculation of Information Gain, petal length (cm) was confirmed as the most discriminative feature for the initial split. The visualizations of the decision tree and its boundaries provide an intuitive and clear representation of the model's classification logic, confirming its effectiveness in partitioning the feature space to classify the different Iris species.

## REFERENCES

- [1] J. Karim et al., "Detection of non-cardiac fetal abnormalities by ultrasound at 11–14 weeks: systematic review and meta-analysis," *Ultrasound Obstet. Gynecol.*, vol. 64, no. 1, pp. 15–27, Jul. 2024.
- [2] Q. Yang et al., "Multi-Center Study on Deep Learning-Assisted Detection and Classification of Fetal Central Nervous System Anomalies Using Ultrasound Imaging," arXiv:2501.02000, Jan. 2025.
- [3] Cochrane Pregnancy and Childbirth Group, "Accuracy of first- and second-trimester ultrasound scan for identifying fetal anomalies in lowrisk and unselected populations," *Cochrane Database Syst. Rev.*, no. CD014715, May 2024.
- [4] H. Bashir, A. Khan, and S. Farooq, "Concept-Bottleneck Models for Explainable Deep Learning in Fetal Ultrasound," in *Proc. IEEE Int.* Symp. Biomed. Imaging (ISBI), Nice, France, Apr. 2025, pp. 123–130.
- [5] F. Serra et al., "Diagnosing fetal malformations on the 1st trimester ultrasound: a paradigm shift," Poster, FMF, 2024.
- [6] K. V. Kostyukov et al., "Deep Machine Learning for Early Diagnosis of Fetal Neural Tube Defects," in World Congress Fetal Medicine, 2025, pp. 21–22.

- [7] T. Tenajas, L. Chen, and M. Rodriguez, "AG-CNN: Attention-Guided Convolutional Neural Networks for Improved Organ Segmentation in Prenatal Ultrasound," in *Proc. IEEE/CVF Conf. Comput. Vision Pattern Recognit. Workshops (CVPRW)*, Seattle, WA, Jun. 2025, pp. 678–686.
- [8] A. Kumar, S. Patel, and D. Rao, "Grad-CAM-Equipped CNN for Renal Anomaly Prediction in Prenatal Ultrasound," in *Proc. IEEE Int. Conf. Med. Image Anal. (MIA)*, Berlin, Mar. 2025, pp. 342–349.
- [9] R. Singh et al., "Attention-Guided U-Net++ with Grad-CAM++ for Robust Fetal Head Segmentation in Noisy Ultrasound Images," Sci. Rep., vol. 15, Art. 19612, Jun. 2025.
- [10] O. O. Agboola *et al.*, "Deep Learning Approaches to Identify Subtle Anomalies in Prenatal Ultrasound Imaging," *Path of Science*, vol. 11, no. 6, pp. 3019–3026, Jun. 2025.
- [11] G. C. Christopher et al., "Enhanced Fetal Brain Ultrasound Image Diagnosis Using Deep Convolutional Neural Networks," EasyChair Preprint, Nov. 2024.
- [12] U. Islam *et al.*, "Fetal-Net: Enhancing Maternal-Fetal Ultrasound Interpretation through Multi-Scale Convolutional Neural Networks and Transformers," *Sci. Rep.*, vol. 15, Art. 25665, Jul. 2025.
- [13] S. Belciug et al., "Pattern Recognition and Anomaly Detection in Fetal Morphology Using Deep Learning and Statistical Learning (PAR-ADISE): Protocol for an Intelligent Decision Support System," BMJ Open, vol. 14, Art. e077366, Feb. 2024.
- [14] K. Ramesh, P. Mehta, and A. Sharma, "A Three-Stage Deep Ensemble Pipeline for Intrapartum Head-Position Assessment in Fetal Ultrasound," in *Proc. IEEE Int. Conf. Image Process. (ICIP)*, Toronto, Sep. 2025, pp. 845–852.
- [15] S. Gupta et al., "Prenatal Diagnostics Using Deep Learning: Dual Approach to Plane Localization and Cerebellum Segmentation," J. Med. Imaging Anal., vol. 7, no. 1, pp. 45–55, Feb. 2025.
- [16] X. Zhang *et al.*, "Advancing Prenatal Healthcare by Explainable AI Enhanced Fetal Ultrasound Image Segmentation Using U-Net++ with Attention Mechanisms," *Sci. Rep.*, vol. 15, Art. 30012, Jun. 2025.